A 0.35-μm subthreshold CMOS ASIC for a Smart Contact Lens Eye-Tracker

Loïc Massin, Fabrice Seguin, Vincent Nourrit, Emmanuel Daniel, Camilla Kärnfelt, Jean-Louis de Bougrenet de La Tocnaye, Cyril Lahuec

A 0.35-μm subthreshold CMOS ASIC for a Smart Contact Lens Eye-Tracker

Loïc Massin, Fabrice Seguin, Vincent Nourrit, Emmanuel Daniel, Camilla Kärnfelt^{+},
Jean-Louis de Bougrenet de la Tocnaye, Cyril Lahuec
Optics Department, Microwave Department^{+}, IMT Atlantique
Brest, Brittany, France
Email: name.surname@imt-atlantique.fr

***Abstract*—This paper describes a camera-less eye-tracker using an instrumented contact lens fitted with photodetectors and illuminated by eyewear. The gaze direction is computed on the lens using the photo-currents by means of a mixed signal 0.35-μm CMOS ASIC. NFC is used to power the ASIC and to transmit the gaze direction to the eyewear. Experimental measurements are performed using a prototype scleral contact lens mounted on a mock-up eye. The measurements show that an accuracy of 0.2° is achievable, i.e. 2.5 times better than current mobile video-based eye-trackers, for a power consumption of 170 μW. Several tests were carried out on several ASICs, demonstrating system reliability despite process variations, operating time, and supply voltage variations.**

I. Introduction

Eye gaze analysis has become a common tool in many fields from cognitive science to human-computer interactions passing by medical diagnosis [1], driver assistance [2] and head-mounted displays with augmented/virtual reality [3].

Video-based eye-trackers are nowadays the most widely used [4]. Images of infrared (IR) illuminated eyes captured by one or several camera(s) are processed to compute the gaze direction [5], [6]. The video-based approach owns its success to its non-invasive nature and constant progress in terms of imaging, computing power and image processing.

Various imaging conditions (camera resolution, iris color, lighting conditions, etc.) can significantly decrease performances. Moreover, the necessary powerful computers and fast cameras make them difficult to integrate in demanding environments. Accurate gaze tracking typically requires head immobilization, the use of several cameras and IR sources, or lengthy calibration [1], [4]. Thus, over the last decade, the reported accuracy of head mounted eye-trackers remained above 0.5° [1], [4], [7], [8], [9].

An approach to improve gaze tracking accuracy is the integration of functions in scleral contact lens (SCL). For instance, a method based on a laser encapsulated into an SCL was proposed in [10]. The operating principle has been established, but results remain preliminary. This paper focuses on the camera-less method [11], [12]. In this system, photodetectors (PTDs), encapsulated into an SCL, are illuminated by an IR source placed on the eyewear. The gaze direction is computed using the PTDs response by an integrated circuit (ASIC) implemented into the lens and powered by an inductive link. The result is then wirelessly sent to the eyewear by near-field communication (NFC). The eye being never idle even during fixations, a sampling rate of at least 200 Hz is required [13], having a significant impact on power consumption.

This paper presents simulations and experimental results of the eye-tracker prototype, with the ASIC, fabricated in AMS 0.35-μm CMOS technology, encapsulated in a lens. The measured accuracy is 0.2° and its stability versus operating time, process, and voltage supply variations is investigated.

This paper is organized as follow. The operation principle of the proposed eye tracker is described in Section II. Section III provides system architecture details. In section IV, experimental measurements are presented and discussed. Section V summarizes system performance and deals with human safety. Finally, Section VI concludes the paper.

II. Operation Principle of the Proposed System

A. Eye Tracking System Geometry

The eyeball is modeled as a sphere of 13 mm radius with its center of rotation as the coordinates origin O. Eye orientation is thus defined by angle θ around z-axis and angle φ around x-axis, Fig. 1(a). A $\pm 16^\circ$ field of view is considered, corresponding to the angular space in which humans prefer moving their eyes rather than their head.

To track the eye movements, 4 PTDs encapsulated into an SCL, Fig. 1(b), are continuously illuminated by a Lambertian IR light source located on the eyewear at $d_0 = 13$ mm (common eye-to-eyewear distance) [12]. PTDs coordinates are $\Theta_0 + \theta$ and $\Phi_0 + \varphi$, where Θ_0 and Φ_0 are the initial angles when $\theta = \varphi = 0^\circ$. PTD#$i$ response is a photo-current I^i_{ph} depending on the received light irradiance E_i in W/m^2, PTD photosensitive surface area and sensitivity. As PTDs move when the eye rotates, I^i_{ph}s change according to gaze direction.

B. Barycenter Calculation

Based on PTDs response, the gaze direction is calculated by means of a barycenter [11]. The barycenter horizontal coordinate with the SCL configuration Fig. 1(b) is given by Eq. 1 (similar equation is used for $\varphi_{\text{computed}}$):

$$\theta_{\text{computed}} = K\Theta_0 \frac{(I^1_{\text{ph}} - I^4_{\text{ph}}) + (I^2_{\text{ph}} - I^3_{\text{ph}})}{I^1_{\text{ph}} + I^2_{\text{ph}} + I^3_{\text{ph}} + I^4_{\text{ph}}}. \quad (1)$$

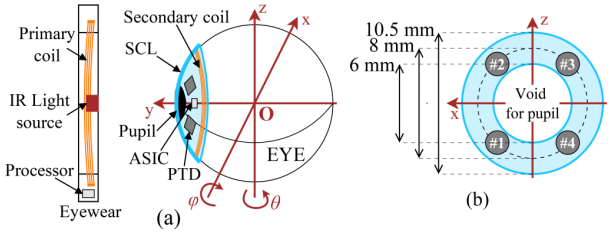

Fig. 1. (a) Proposed system: IR source on the eyewear illuminates PTDs encapsulated into a SCL. Eye tracking data is computed on the lens by an ASIC and wirelessly transmitted to the eyewear. (b) Flexible substrate dimensions and PTDs configuration, fitting into a 16.5 mm diameter SCL.

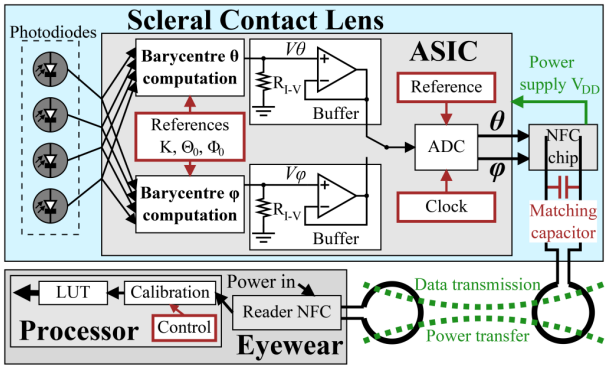

Fig. 2. Gaze tracking system architecture. All on-lens components must be on the flexible substrate of Fig. 1(b) and fit into a 850 μm thick cavity.

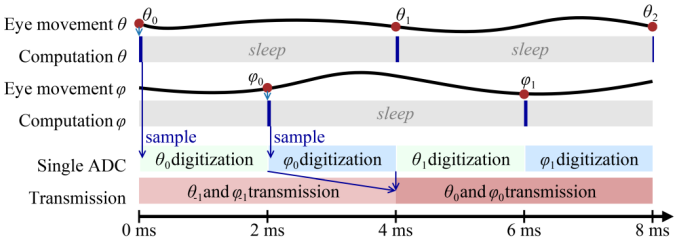

Fig. 3. Timing diagram for the proposed system. Barycenter computing units continuously compute θ_{computed} and $\varphi_{\text{computed}}$ wich are sequentially digitized at 500 Hz.

K is a slope factor taking into account the illumination profile and PTDs disposition. Constant $K\Theta_0$ thus converts a barycentric variation to an angle in degrees [12]. Difference between θ_{computed} and the actual θ, θ_{error}, gives the accuracy.

C. Calibration and Robustness of the System

Misplacement of SCL and eyewear at system setup, and the ASIC introduce systematic error that need correction. The induced piecewise linear error is canceled by a 5-points calibration [11]:

1) 1-point for offset correction. The user is asked to look straight ahead, $\theta = \varphi = 0^\circ$. Then, the two offset errors, for θ and φ, are recorded and subtracted from all computed angles.

2) 2-points by direction for gain correction. Depending on the barycenter sign, a corrective gain G_- is applied for negative results, and a gain G_+ otherwise. For these adjustments, the user is asked to look at known angles: $\pm 16^\circ$ in the θ direction, and likewise for φ. A slope calculation between -16° and 0° yields the gain G_-, and between 0° and +16° for G_+.

After calibration, ambient light, eyewear displacement and lens slippage may degrade the accuracy. PTDs peak sensitivity to the IR source and differential computation mitigate the impact of ambient parasitic lighting. The eyewear is firmly strapped to the head to prevent displacement. Finally, an SCL slides only slightly once inserted and its position stabilizes after 1.5 h [14]. Additionally, an inherent non-linear error, due to the spherical aspect of the problem, limits accuracy. As this error is predictive, the correspondence between the computed θ_{computed} and the actual θ is tabulated in a table pre-filled by means of a theoretical study [11].

III. Description of System Implementation

A. System Architecture Considerations

The system architecture, Fig. 2, is designed to meet volume, power and accuracy constraints. Thus, the calibration and the tabulated correction for inherent error cancellation, implemented as a lookup table (LUT), are located on the eyewear where power and space are not limited. An ASIC implements all on-lens functions. As barycenter computation is performed on-lens, only the two computed directions are digitized by a single ADC, limiting power consumption. A 12-bit ADC and LUT are chosen to ensure that the resolution does not degrade the accuracy of the system. The wireless link between the on-lens system and the eyewear is done by an off-the-shelf NFC chip, the NTAG NT3H1101 from NXP [11], having suitable dimension to fit into an SCL. Exciting the primary coil with 140 mW at 13.56 MHz at a distance of 13 mm, the NXP NTAG associated with a lens-size secondary coil harvests 0.92 mW. The chip consumes 0.28 mW for its own operation.

B. Temporal Constraints

Temporal accurate tracking requires a continuous gaze sampling rate higher than 200 Hz. Based on the NXP NTAG datasheet, data transmission requires 4 ms, limiting system sampling rate at 250 Hz. Considering the computation time for the analog barycenter computing circuit negligible (ns) compared to these 4 ms, the ADC must digitize each direction at most in 2 ms (one by one), i.e. a data rate of at least 500 Hz.

C. ASIC Implementation and Simulation

A 0.35-μm CMOS process from AMS is chosen for circuit implementation with a voltage supply V_{DD} of 1.8 V. To limit power consumption, subthreshold biased MOS transistors are used as much as possible. The drawback of this approach is its high sensitivity to fabrication process variations and to transistors mismatches. To limit the impact of these variations, cascode current mirrors, large transistors and centroid layout are used. The calibration corrects the residual error.

The ASIC architecture is depicted in Fig. 2. The barycenter is computed by two current-mode analog circuits equivalent

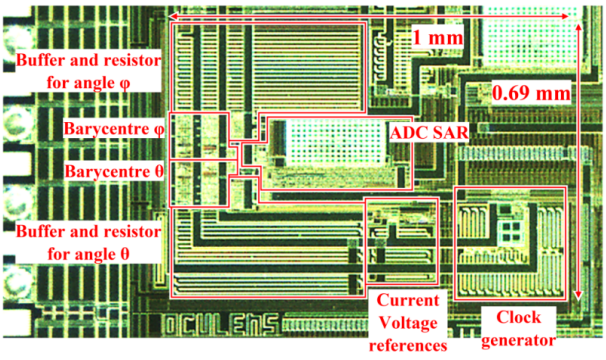

Fig. 4. Microphotograph of the eye tracking circuit implemented in a multi-projects die.

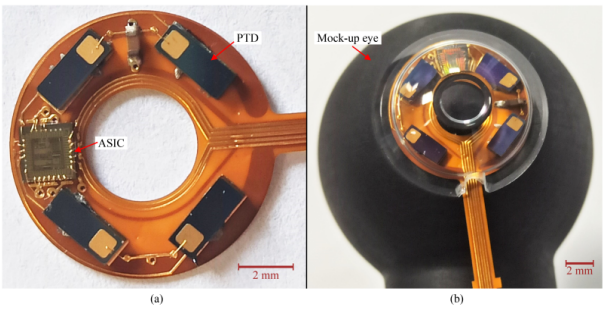

Fig. 5. Prototype SCL fabricated embedding the ASIC and 4 PTDs.

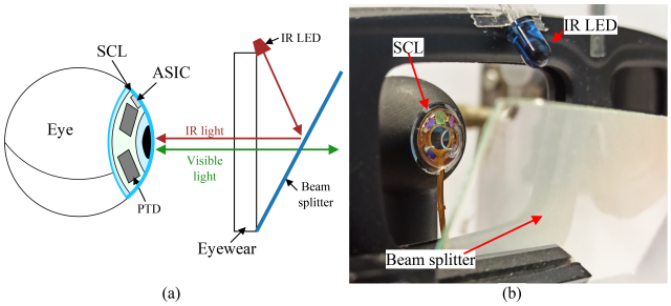

Fig. 6. Test bench for ASIC measurements with IR source on the eyewear.

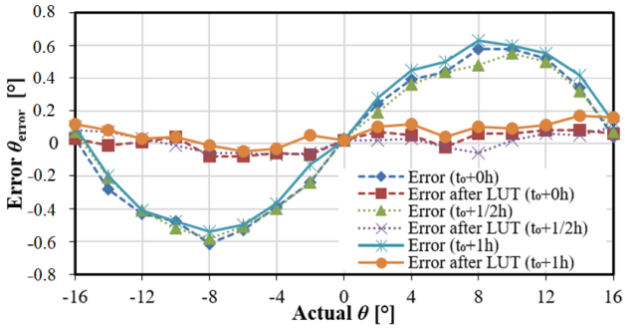

Fig. 7. Measured accuracy stability over time. Calibrated once at time t_0. Accuracy remains stable for 1h without re-calibration.

to that in [15], one per direction, directly fed by photo-currents from PTDs and is digitized by a 12-bit successive approximation register ADC (SAR ADC). The operating frequency is 12.5 kHz, provided by a 400 kHz Wien bridge harmonic oscillator divided by 32. Since the barycenter is output as a current and the SAR ADC is voltage mode, an 1 MΩ resistor $R_{I\text{-}V}$ performs the current-to-voltage conversion, having a linear response over a wide dynamic range. In addition, a subthreshold folded-cascode amplifier implements an unity gain buffer for impedance matching.

MC analyses using I^i_{ph}s measured on a prototype provides realistic ASIC simulations. After calibration and LUT compensation, the simulated system accuracy is 0.2°, with a power consumption of around 170 μW.

IV. Experimental Measurements

A. Prototype Scleral Contact Lens

The fabricated multi-projects ASIC is shown in Fig. 4 and the circuit dedicated to the eyetracker occupies 0.69 mm^2 of silicon area. The ASIC and the 4 Silonex SLCD-61N8 PTDs are bonded on a 0.2 mm thick flexible substrate, Fig. 5. These 0.4 mm-thick IR PTDs dimensions are 1.3 by 3.4 mm with a photosensitive surface area of 2.7 mm^2. The bonded ASIC and PTDs are encapsulated in a 16.5 mm diameter SCL. The prototype is mounted on an artificial eye rotating $\pm 16^\circ$ for angle θ.

The SCL is illuminated by an IR LED (Vishay TSAL6100) at $\lambda = 940$ nm associated with a beam splitter placed on the eyewear so that the IR source is not in the field of view, Fig. 6.

For test purpose, the ASIC is wire connected to a Raspberry Pi 3 b+ card via a ESP32 micro-controller (for data format adpatation). A Python program acquires data, performs calibration and applies the LUT correction. This set-up does not add extra latency. The NFC chip is not encapsulated into the SCL.

B. Eyetracker Accuracy with CMOS Process Variations

Once the system is powered up, calibration as described in Section II.C is done. The digitized θ_{computed} angle is acquired for actual θ angles from -16° to +16° by step of 2°. The LUT correction is applied in real-time to each θ_{computed}. This is performed three times after calibration: immediately after, half an hour after and one hour after to check the stability of the measurement and its reproducibility over time without re-calibration.

Thanks to calibration, θ_{error} is the inherent error of the method, Fig. 7. After applying the LUT correction, the system accuracy is 0.2°, 2.5 times better than state-of-the-art mobile video-based eye-trackers. In addition, the accuracy remains the same over the three measurement series: performance is not degraded after 1 h of operation. Also, electronic noise and ambient ligh impact the precision. The measured precision is consistently 0.04°, obtained by repeating acquisition 100 times for each θ angles.

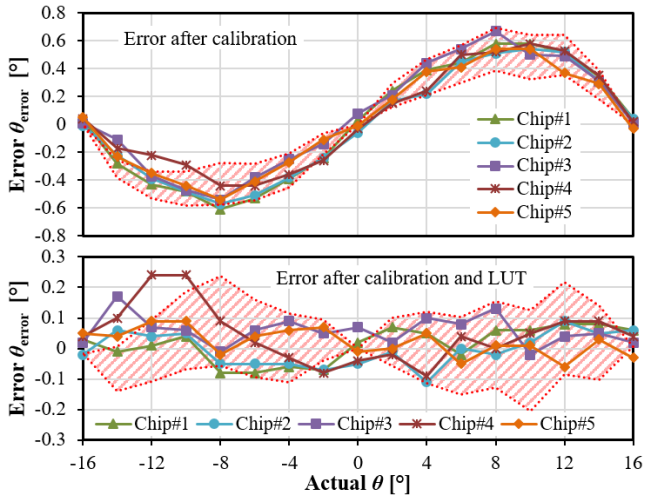

Fig. 8. Measured accuracy stability versus process variations for 5 ASICs. Results in line with MC analysis (hatched area) .

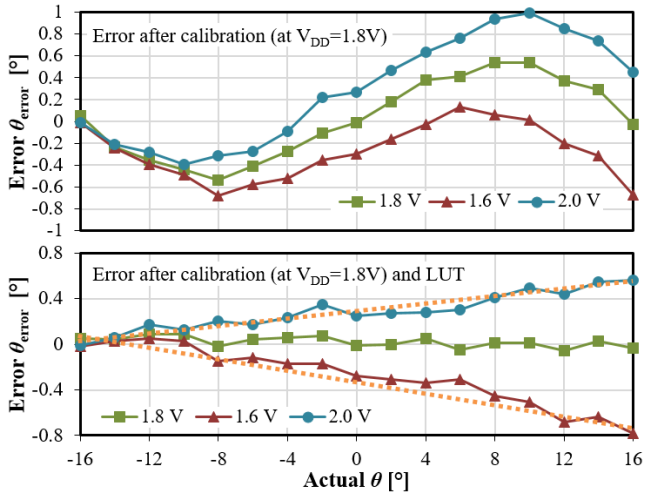

Fig. 9. Measured accuracy versus supply voltage V_{DD} variation. The system is first calibrated for a nominal V_{DD} of 1.8 V. Then, for each angle θ, the accuracy is measured for the nominal V_{DD} and a $\pm$10% variation, introducing a linear error (trend line in dotted).

The robustness of the system with process variations is shown by measuring the accuracy for 5 ASICs, Fig. 8. The accuracies is at most 0.2° after LUT correction, similar to that obtained from MC analysis.

C. Eyetracker Accuracy with On-lens Voltage Variations

The voltage supply will fluctuate with the movements of the lens-size secondary coil on the SCL with respect to the primary one as the eye moves when powered by NFC. The ASIC accuracy with supply voltage variations was measured.

First, the system was calibrated once at the nominal supply voltage of 1.8 V. Then, for each angle θ, three measurements were performed: for the nominal V_{DD} of 1.8 V, and for $\pm$10% variations (1.6 V and 2.0 V), Fig. 9. This voltage supply variations decreases accuracy, increasing error up to -0.8°, similar to video-based eye-trackers.

TABLE I
MEASURED PERFORMANCE SUMMARY

	This work	Tobii Pro Glasses 2 [7]	Pupil Labs glasses [8]
Approach	Smart lens (based on ASIC measurements on a test bench)	Video-based (worn by an user in controlled environment)	Video-based (worn by an user in controlled environment)
Accuracy	0.2°	0.5°	0.82°
Precision	0.04°	0.3°	0.31°
Calibration decay	No error increase after 1 h	Unknown	Error increase by 0.25° after 5 min
Sample rate	250 Hz	100 Hz	240 Hz

V. System Summary

A comparison between the proposed eye-tracker and modern mobile video-based eye trackers is presented in Table I. The SCL eye-tracker offers a better accuracy and precision than video-based ones. In addition, the sample rate is at the top of state-of-art for mobile eye-tracking.

The ASIC consumes 0.17 mW (92 and 1.4 μA for the analog and digital part, respectively, at V_{DD} = 1.8 V), well below the 0.92 mW the NXP NTAG NT3H110 supply capacity. Adding the NXP NTAG power consumption, the overall on-lens system consumes 0.45 mW.

The presented results are obtained on a mock-up eye and need to be confirmed on a real eye. Nevertheless, the results demonstrate the system validity. Moreover, the encapsulated ASIC can be powered by a contact lens size compatible NFC system (NXP TAG and secondary coil) [16].

Regarding human safety, bio-compatibility is guaranteed by encapsulating all components in a medical SCL. Resting on the sclera, the lens creates a tear-filled vault between the SCL and the cornea, avoiding eye dryness. The measured irradiance E_i of the IR source at the lens surface is less than 20 μW/mm^2, compliant with ocular safety standards for near-IR lighting [17]. Finally, since a specific absorption rate of 0.021 W/kg was obtained from a 2 W power source in [18], well below the maximum 2 W/kg allowed, the 140 mW NFC power source used here insure human safety.

VI. Conclusion

An accurate eyetracker based on an instrumented SCL has been validated in this paper. The on-lens ASIC, fabricated in an AMS 0.35-μm CMOS technology, along with photodiodes, were encapsulated in an SCL mounted on a mocked-up eye. The system achieves an accuracy of 0.2°, 2.5 times better than state-of-the-art mobile video-based eye-trackers. No periodic calibration is required. The power consumption of 170 μW is compliant with NFC constraints. Further validation on a real eye are required.

Acknowledgment

The authors thank LCS (an ISO 13485 Medical Devices certified company manufacturing and selling scleral contact lenses) for fabricating the prototype lens.

REFERENCES

[1] A. J. Larrazabal, C. E. Garcia Cena, and C. E. Martinez, "Video-oculography eye tracking towards clinical applications: A review", *Comput. Biol. Med.*, vol. 108, Mar. 2019, pp. 57–66.

[2] F. Vicente, Z. Huang, X. Xiong, F. De la Torre, W. Zhang, and D. Levi, "Driver Gaze Tracking and Eyes Off the Road Detection System", *IEEE Trans. Intell. Transp. Syst.*, vol. 16, no. 4, Aug. 2015, pp. 2014–2027.

[3] A. Plopski. Y. Itoh, C. Nitschke, K. Kiyokawa, G. Klinker, and H. Takemura, "Corneal-Imaging Calibration for Optical See-Through Head-Mounted Displays", *IEEE Trans. Visual Comput. Graphics*, vol. 21, no. 4, Apr. 2015, pp. 481–490.

[4] A. Kar, and P. Corcoran, "A Review and Analysis of Eye-Gaze Estimation Systems, Algorithms and Performance Evaluation Methods in Consumer Platforms", *IEEE Access*, vol. 5, Sep. 2017, pp. 16495–16519.

[5] A. Villanueva, and R. Cabeza, "A Novel Gaze Estimation System With One Calibration Point", *IEEE Trans. Syst. Man Cybern. Part B Cybern.*, vol. 38, no. 4, Aug. 2008, pp. 1123–1138.

[6] X. Zhang, Y. Sugano, M. Fritz, and A. Bulling, "MPIIGaze: Real-World Dataset and Deep Appearance-Based Gaze Estimation", *IEEE Trans. Pattern Anal. Mach. Intell.*, vol. 41, no. 1, Jan. 2019, pp. 162–175.

[7] M. Cognolato, M. Atzori, and H. Müller, "Head-mounted eye gaze tracking devices: An overview of modern devices and recent advances", *Journal of Rehabilitation and Assistive Technologies Engineering*, vol. 5, Jun. 2018, pp. 1–13.

[8] B. V. Ehinger, K. Groß, I. Ibs, and P. König, "A new comprehensive eye-tracking test battery concurrently evaluating the Pupil Labs glasses and the EyeLink 1000," *PeerJ* 7:e7086, 1-43 (2019).

[9] C. H. Morimoto, and M. R.M. Mimica, "Eye gaze tracking techniques for interactive applications", *Computer Vision and Image Understanding*, vol. 98, no. 1, Apr. 2005, pp. 4–24.

[10] A. Khaldi, E. Daniel, L. Massin, C. Kärnfelt, F. Ferranti, C. Lahuec, F. Seguin, V. Nourrit, and J.-L. de Bougrenet de la Tocnaye, "A laser emitting contact lens for eye tracking", *Sci Rep*, vol. 10, no. 1, Sep. 2020, pp. 14804.

[11] L. Massin, F. Seguin, V. Nourrit, E. Daniel, J.-L. de Bougrenet de la Tocnaye, and C. Lahuec, "Smart Contact Lens Applied to Gaze Tracking", *IEEE Sensors*, vol. 21, no. 1, Jan. 2021, pp.455–463.

[12] L. Massin, V. Nourrit, C. Lahuec, F. Seguin, L. Adam, E. Daniel, and J.-L. de Bougrenet de la Tocnaye, "Development of a new scleral contact lens with encapsulated photodetectors for eye tracking", *Optics Express*, vol. 28, no. 19, Sep. 2020, pp. 28635–28647.

[13] R. Andersson, M. Nyström, and K. Holmqvist, "Sampling frequency and eye-tracking measures: how speed affects durations, latencies, and more", *Journal of Eye Movement Research*, vol. 3, no. 3, Jun. 2010, pp. 1–12.

[14] S.J. Vincent, D. Alonso-Caneiro, and M.J. Collins, "The temporal dynamics of miniscleral contact lenses: Central corneal clearance and centration", *Contact Lens Anterio.*, vol. 41, no. 2, Apr. 2018, pp. 162–168.

[15] C. Lahuec, and M. Arzel, "An analog core computing the center of pressure in a knee replacement prosthesis", *IEEE 9th International New Circuits and systems conference*, 2011, pp. 105–108.

[16] L. Massin, C. Lahuec, F. Seguin, V. Nourrit, and J.-L. de Bougrenet de la Tocnaye, "Multipurpose Bio-Monitored Integrated Circuit in a Contact Lens Eye-Tracker", *Sensors*, vol. 22, no. 2, Jan 2022, pp. 595.

[17] ICNIRP, "Guidelines on limits of exposure to incoherent visible and infrared radiation", *Health Phys.*, vol. 5, no. 1, 2013, pp. 74–96.

[18] Y. Kim, J. Maeng, and P.P. Irazoqui, "Eyeglasses-powered, contact lens-like platform with high power transfer efficiency", *Biomed Microdevices*, vol. 17, no. 75, Jul. 2015, pp. 1–9.